JAERI-M
8205

STUDY ON VERY-LOW-Q DISCHARGES IN DIVA

April 1979

DIVA Group
Division of Thermonuclear Fusion Research

日本原子力研究所
Japan Atomic Energy Research Institute

JAERI-M 8205

Study on Very-Low-q Discharges in DIVA

DIVA Group

Division of Thermonuclear Fusion Research
Tokai Research Establishment, JAERI

(Received March 20, 1979)

Confinement and mhd characteristics of very-low-q discharges were studied in DIVA/JFT-2a. It is shown that plasmas with good confinement property are obtained with $1.3 \leq q_a \leq 2$ and no current disruption can be excited in discharges with $q_a \lesssim 2$. Application of the very-low-q discharges having these attractive characteristics to a large device is discussed.

Keywords: DIVA Tokamak, Low-q Discharges, Confinement, MHD Stability, Disruption

JAERI-M 8205

DIVAにおける極低安全系数放電の研究

日本原子力研究所東海研究所核融合研究部
DIVAグループ

（1979年3月20日受理）

DIVA／JFT－2aにおいて極低安全系数放電の閉じ込めおよび磁気流体的性質についての研究を行なった。良い閉じ込め特性をもったプラズマが $1.3 \leq q_a \leq 2$ において得られること，および，$q_a < 2$ において電流ディスラプションを励起できないことを示した。また，このようにすぐれた性質をもった極低安全系数放電の大型装置への適応についても述べる。

CONTENTS

目　　次

1. Introduction

In order to obtain a high-β tokamak, it is one of the most atractive methods to realize a stable low-q discharge. A stable very-low-q discharge, i.e. $q_a < 2$, is theoritically expected in a tokamak with a close shell. In experiment, very-low-q discharges were obtained in T-6 having a conducting wall near the plasma column but detailed investigation was not done.[1] In DIVA, it was suggested that q_a can be easily decreased as decreasing impurity level by the poloidal divertor.[2] Recently very-low-q discharges are obtained after controlling radiation loss by employing the divertor or pure titanium walls in* DIVA and results are briefly reported in ref. (3). This paper reports detailed results. In the following section, experimental conditions and diagnostics are described. Confinement characteristics and mhd characteristics are given in section 3 and section 4, respectively. Summary is given in section 5.

2. Experimental Conditions and Diagnostics

DIVA is a small tokamak with a close shell coated with gold or titanium.[4] In this study, discharges are mainly obtained without the poloidal divertor and with pure titanium walls. Two rail limiters having titanium surfaces are mainly employed to define the plasma current channel. The plasma has non circular cross section, and the effective radius is determined by $\bar{a} = l_p/2$, where l_p is a circuit length of the noncircular cross section. Thus determined effective radius of the shell $\bar{b}$ is 12 cm and that of the plasma $\bar{a}$ is 10 cm at the usual case of distance between the limiter and the shell surface $\bar{d}_1 = 2.0$ cm. The major radius R of the DIVA is 60 cm. Generally defined q_a is employed, i.e. $q_a = (\bar{a}/R)(B_T/\bar{B}_p)$ where $\bar{B}_p = I_p/2\,\bar{a}$. Therefore the defined safety factor q_a is that for a straight column and a safety factor $q_a{}^t$ including toroidal effect is a few percent larger than the defined value.[5]

In order to reduce both gas and metal impurities, about 500 mg of titanium is evaporated from 10-16 titanium balls distributed in the vacuum chamber before starting each 60 discharges. The base pressure is less than 3×10^{-8} torr, the main composition of residual gas is hydrogen and level of other compositions is less than 10 %. Hydrogen gas is supplied from three fast acting pulse-valve and a programmed valve before and during a discharge.

The maximum toroidal field is 2 T in the device but is 1.5 T in this low-q experiment because of the saturation of the iron transformer, i.e. the maximum plasma current is 80 kA without the divertor and 55 kA with the divertor. Therefore very-low-q discharges are mainly investigated without the divertor. Plasma position is controlled by d.c. vertical and horizontal field and the close copper shell with thickness of 2-3 cm.

In addition to conventional measurements, following measurements are made to investigate effects of the sawtooth oscillations: 1) electrostatic probe measurements in the scrape-off layer; 2) a laser beam for Thomson scattering is triggered by a sawtooth signal in order to obtain time variation of electron temperature profiles according to the sawtooth oscillations.

3. Confinement Characteristics of Very-Low-q Discharge

The confinement study is always importance in fusion oriented research, because it is meaningless to obtain a plasma without a good confinement property. Therefore it is one of the most important terms to investigate the confinement characteristics also in the very-low-q experiment. In this section, confinement characteristics of very-low-q discharges are described.

Very-low-q discharges with a good confinement property are obtained with $q_a \geq 1.3$, i.e. average energy confinement time is dominated by sawtooth oscillations but Alcator scaling continues to hold with a higher numerical factor in front of $a^2\bar{n}_e q_a^{1/2}$ when $q_a \geq 1.3$. It is shown that suppression of the sawtooth oscillations is important and desirable because the energy confinement time has a posibility to increase by a factor of a few by suppressing the oscillations.

In the following sub-section, experimental results are shown and in 3.2, conclusions are given.

3.1 Experimental Results

Figure 3.1 shows measured radiation loss power v.s. plasma current: (●) corresponds to discharges with gold walls without the divertor, (○) with gold walls and the divertor and (△, ▲) with titanium walls in this experiment. The radiation loss power is very low, typically 10 - 20 %, in this experiment which is the same level to that the poloidal divertor with gold walls.[2] In these discharges with low level of impurities, stable very-low-q plasmas are obtained with good reproducibility.

Typical discharge characteristics with $q_a < 2$ are shown in Fig.3.2, i.e. time behavior of loop voltage V_L and current I_p, and profiles of density n_e, radiation loss power density P_{py} including charge exchange loss and electron temperature at the top and bottom of the sawtooth oscillations. In this case, the maximum plasma current is 63 kA and the minimum q_a value is 1.65. The safety factor q_a decreases to 2 during the first 2.5 ms and is less than 2 during the following 12 ms. A large voltage increase is observed when the plasma current is crossing through $q_a = 2$ and is considered to be induced by $m = 2/n = 1$ kink mode (see section 4) but the current increases smoothly. No current disruption is observed with $q_a < 2$. The discharge characteristics, however, is dominated by large sawtooth oscillations which

are observed not only in X-ray signal or electron temperature but also in the loop voltage as shown in Fig. 3.2. The sawtooth oscillation observed in the loop voltage are due to rearrangement of the current distribution by the internal disraption. The internal disruption reduces electron temperature of the hot column (Fig. 3.2), i.e. about 50 eV decrease in $r \lesssim 7$ cm and 40 eV increase at the plasma boundary. Energy loss by the internal disruption dominates the average energy confinement time. The average energy confinement, however, is 5.7 ms with the plasma radius of only 10 cm and average β is 0.8 % in this case. Therefore it can be mentioned that a $q_a < 2$ discharge is stabely obtained.

The following interest is the minimum q_a value. Figure 3.3 shows a $q_a = 1.3$ discharge which has similar characteristics to those in the $q_a = 1.7$ discharge shown in Fig. 3.2. No large voltage spike is observed also in $q_a \lesssim 1$ discharge as shown in Fig. 3.4 but the average energy confinement time is drastically reduced, i.e. the average confinement time is only about 50 μs at $q_a = 1.05$ with $n_{eo} = 2 \times 10^{13}$ cm^{-3} and $T_{eo} = 130$ eV. This poor confinement time may be due to the wide area of $q < 1$ as discussed below. When q_a is reduced down to 1 or a less value, large increase of the loop voltage which may be due to $m = 1/n = 1$ surface mode is observed and the current cannot increase any more. Therefore it can be said that a good confined plasma is obtained with $q_a \geq 1.3$, a poor confined plasma with $q_a \lesssim 1$ and an unstable discharge with $q_a \lesssim 1$.

Stable plasmas with a good confinement property are obtained with $q_a \geq 1.3$ and confinement properties are investigated in detail. Figure 3.5 shows the radius of $q = 1$ surface as a fanction of q_a. It should be noted that the area of $q < 1$ increases monotonically as decreasing q_a. This result may explains the poor confinement time in the $q_a \lesssim 1$ discharge (Fig. 3.4). Another important result on $q = 1$ surface is deformation of the $q = 1$ surface in a very-low-q discharge (Fig. 3.4), i.e. magnetic surfaces become non circular as decreasing the q_a value because the current profile becomes flat and magnetic surfaces inside a plasma become non circular shape given by the inner surface of the shell. This result shows that the non circular cross sectional tokamak inside the plasma column can be realize in a very-low-q discharge.

Mean plasma density $\bar{n}_e$ and safety factor q_a are summarized in Fig. 3.6 following Murakami scaling.[6] The density limitation has not been investigated in DIVA because of its short discharge duration but the obtained density in high-q discharges is almost comparable to those obtained in

DITE[7] or JFT-2.[8] In very-low-q discharges, obtained density increases, e.g. $\bar{n}_e/(B_T/R_o) = 4 - 5$. Therefore it can be said that the very-low-q discharges are suitable to obtain a high density plasma.

In order to investigate the parameter dependence of the energy confinement time, the following discharges are studied: 1) fixing B_T and $\bar{n}_e$ and changing q_a, i.e. $q_a = 1.8$ and 2.5; 2) fixing B_T and q_a and changing $\bar{n}_e$, i.e. $\bar{n}_e = 1.1 \times 10^{14}$ cm^{-3} and 6×10^{13} cm^{-3}. The results show that the energy confinement time is almost proportional to $\bar{n}_e$ and roughly proportional to $q_a^{1/2}$. Therefore confinement time is well described by Alcator scaling. Confinement time in various discharge conditions are summarized in Fig. 3.7. (▲,△) shows data in this experiment, and (●) without the divertor and (○) with divertor in the previous experiment.[2] The very-low-q discharges seem to increase the energy confinement time because the old confinement time (●) without the divertor is almost equal to Alcator scaling. The previous experiment, however, shows that the energy confinement is improved by reducing impurities as shown by (○).[2] Therefore it seems reasonable that the reduction of impurities improves the energy confinement also in very-low-q discharges and Alcator scaling continues to hold in very-low-q discharges with a higher numerical factor in front of $a^2\bar{n}_e q_a^{1/2}$ not because of low-q effects but because of the reduction of impurities.

The result shows that Alcator scaling continues in the very-low-q discharges which are dominated by internal disruptions. The scaling, however, was obtained in rather-high-q discharges which are not strongly affected by the internal disruption. Therefore the following question arises: why does Alcator scaling continue in the very-low-q discharges? Empirical scaling for sawtooth oscillations firstly obtained in TFR may answer this question and is also obtained in the very-low-q discharges in DIVA, i.e. frequency of the sawtooth oscillation is proportional to $q_a/\bar{n}_e$, the amplitude is roughly proportional to $q_a^{-3/2}$ and consequently energy confinement time dominated by the sawtooth oscillations is proportional to $\bar{n}_e q_a^{1/2}$.

It is very interesting to know the energy confinement time excluded the effects of the internal disruption because the sawtooth oscillations have a possibility to be suppressed in a device with a high power additional heating and because the energy confinement time excluded the effect becomes important. Figure 3.8 shows a typical energy balance in the sawtooth oscillations. The average energy confinement time is 5.7 ms and dominated

by the internal disruptions, i.e. energy loss due to the internal disruptions is the major loss from the plasma column. When X-ray intensity increases, the energy loss is only about 40 J during 0.82 ms and the confinement time is about 20 ms. During the internal disruption, the energy loss is about 125 J during only 0.18 ms and the confinement time is only about 0.8 ms. Therefore the energy confinement time excluded the effects of the sawtooth oscillations is about 20 ms, i.e. the confinement time can be improved by a factor of a few if the sawtooth oscillations are suppressed. And the energy confinement time excluded the internal disruption is much longer than the value gived by Alcator scaling.

The above result suggests that Alcator scaling has to be modified. Alcator scaling describes well the observed data except the numerical factor in front of $a^2\bar{n}_e q_a^{1/2}$ and the previous experiment shows that the numerical factor increases as increasing the radius of the hot column. In the very-low-q discharges, the radius of the hot column is large as shown in Fig. 3.9. Therefore it seems reasonable that the long confinement time during the slow rise of the sawtooth oscillations is explained by the same reason, i.e. the large effective radius gives the long confinement time. Energy confinement time without large mhd activities are summarized in Fig. 3.10 as a function of $\bar{n}_e q_a^{1/2} a_{half}^2$ where a_{half} is a half radius of an electron temperature profile. In the figure, (●) shows old data with gold walls without the divertor, (○) with gold walls with the divertor and (▲) with $q_a < 2$. The modified Alcator scaling describes well the observed confinement time in various discharge conditions.

3.2 Conclusions

Very-low-q discharges are investigated in DIVA and following results are obtained.

1) Stable plasmas with a good confinement properties are obtained with $1.3 \leq q_a < 2$.
2) A $q_a \gtrsim 1$ discharge has a poor confinement time.
3) Non circular configuration inside a plasma column is obtained in the very-low-q discharges.
4) Energy confinement time can be improbed by a factor of a few in very-low-q discharges if the internal disruption is suppressed.
5) Modified Alcator scaling, i.e. $\tau_E \propto a_{half}^2 \bar{n}_e q_a^{1/2}$, describes well observed confinement time of various discharge conditions without large mhd activities where a_{half} is the half radius of an electron temperature profile.

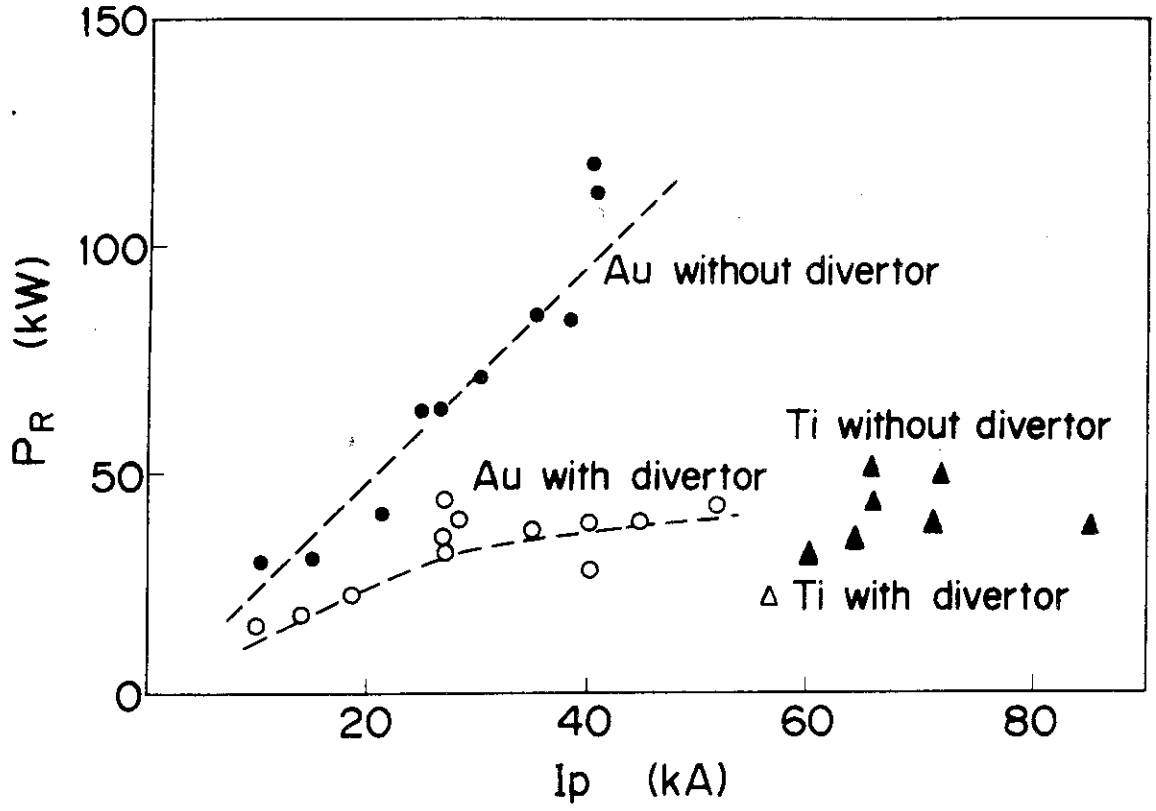

Fig. 3.1 Radiation loss power v.s. plasma current
(△) and (▲) show the present data.

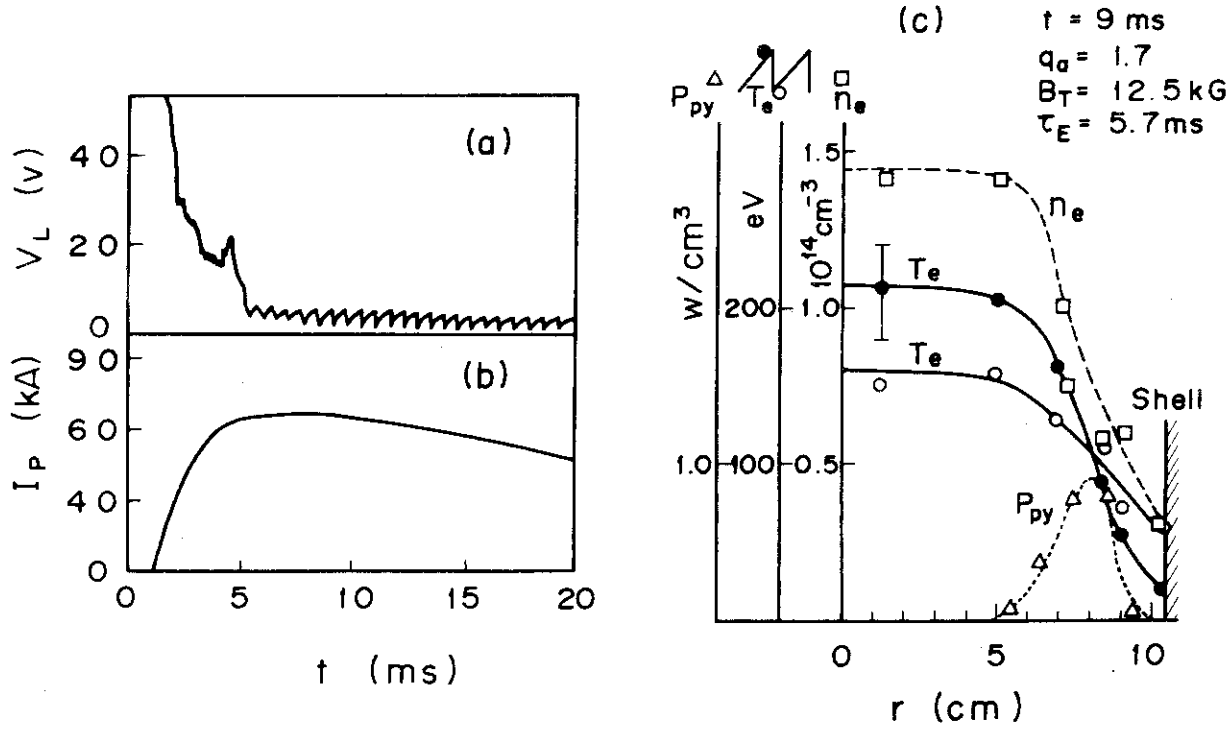

Fig. 3.2 Typical plasma characteristics in a q_a < 2 discharge.

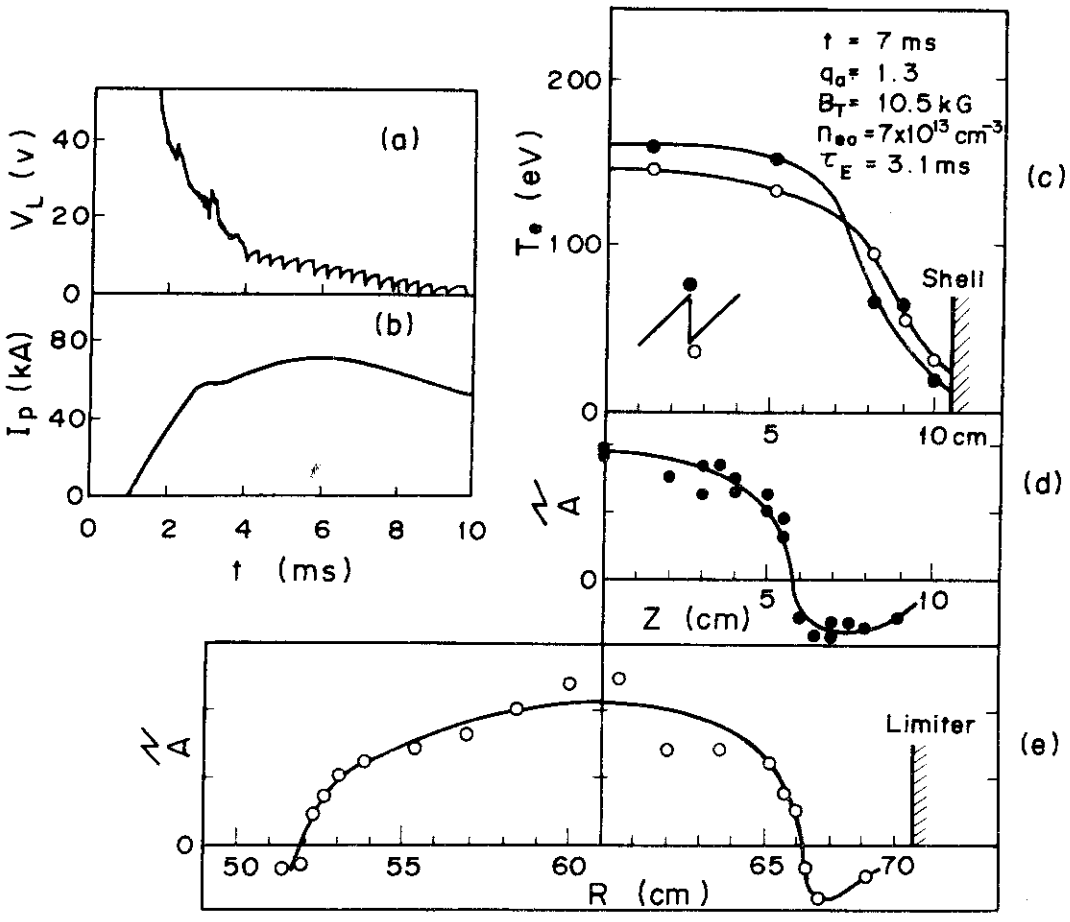

Fig. 3.3 Typical plasma characteristics in a q_a=1.3 discharge

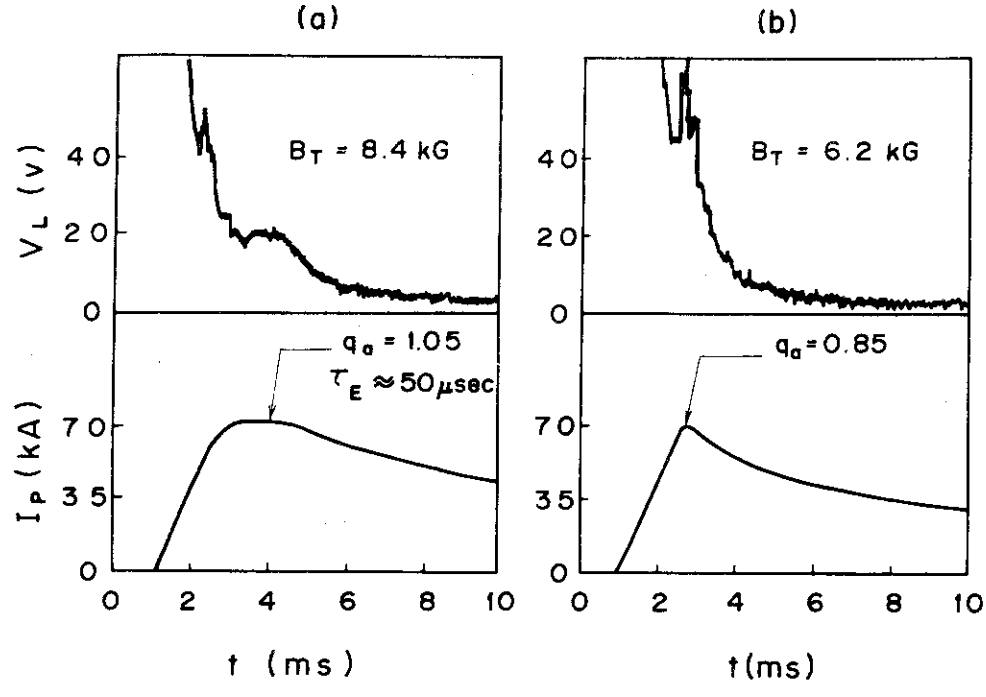

Fig. 3.4 Wave forms of loop voltage and plasma current with q_a=1.05 and 0.85.

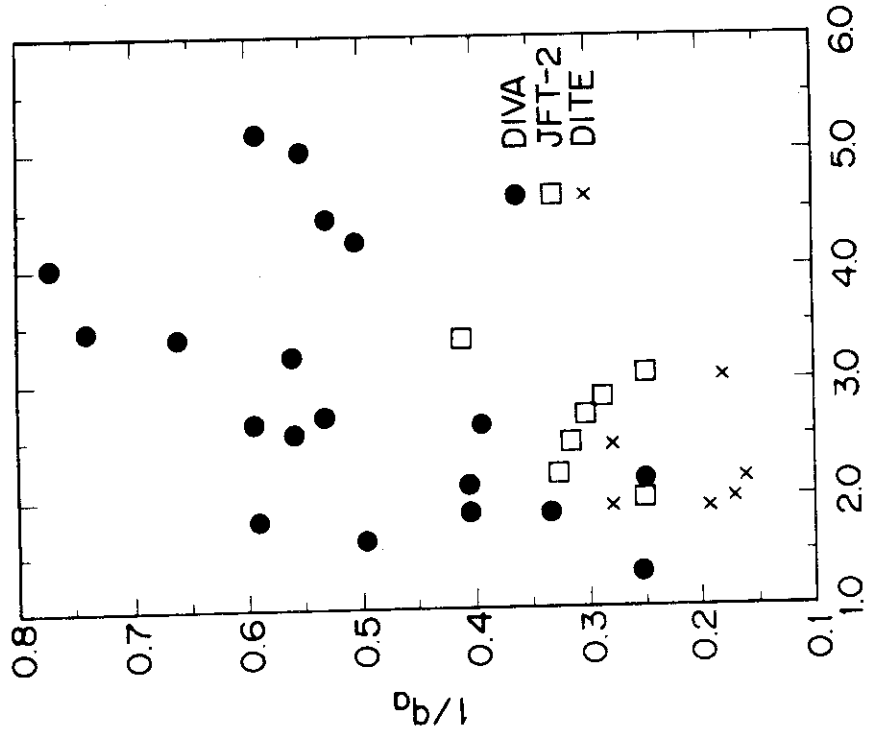

Fig. 3.6 Typical plasma density v.s. $\bar{n}_e/(B_T/R_0)$ where $\bar{n}_e$ is mean electron density in cm^{-3}, B_T toroidal field in T and R_0 major radius in m.

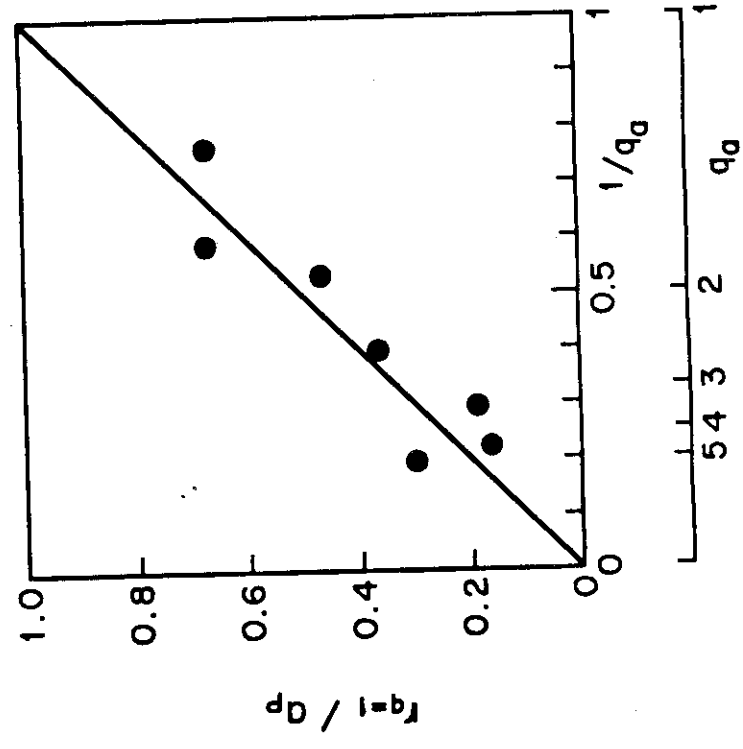

Fig. 3.5 Radius of q=1 surface v.s. q_a.

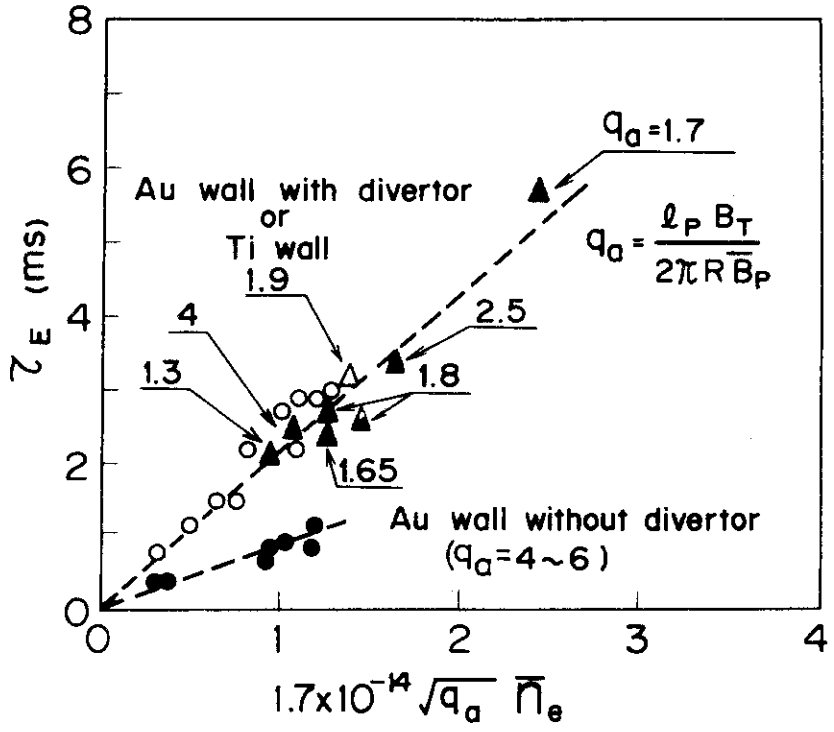

Fig. 3.7 Energy confinement time v.s. $q_a^{1/2}\bar{n}_e$ where $\bar{n}_e$ is mean electron density in cm^{-3}.

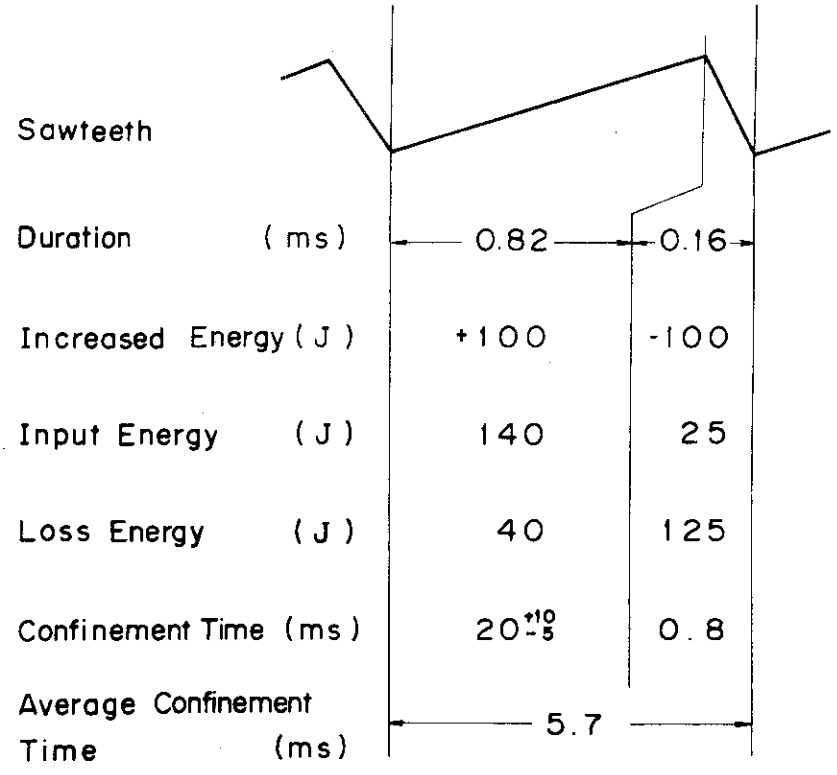

Fig. 3.8 Energy balance in a swatooth oscillation.

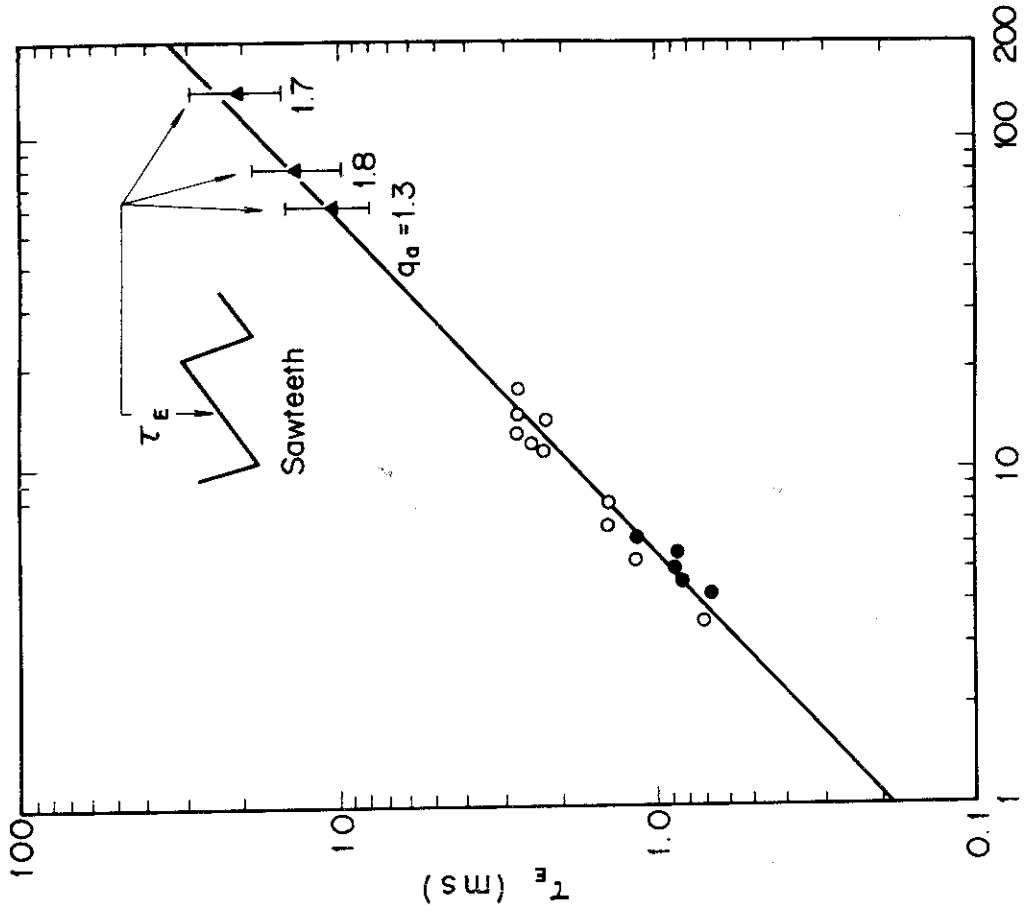

Fig. 3.10 Energy confinement time v.s. $q_a^{1/2} \bar{n}_e a^2_{half}$ where a_{half} is a half radius of an electron temperature profile. Discharge conditions are shown in Fig. 3.1.

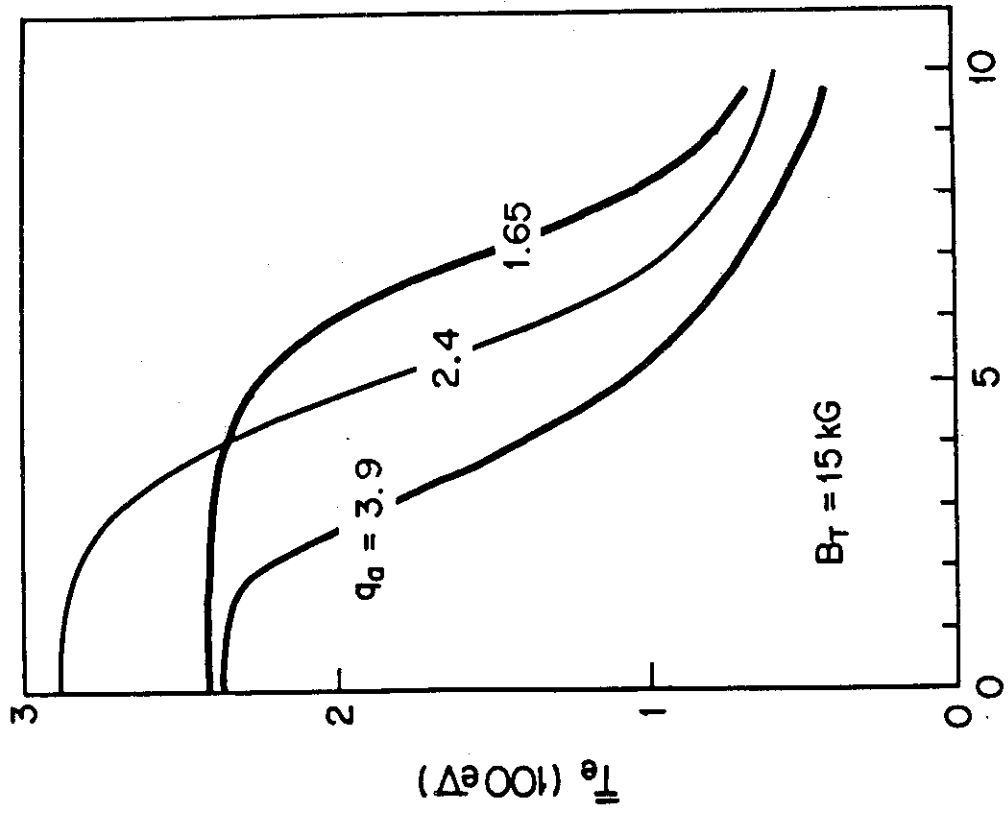

Fig. 3.9 Electron temperature profiles in discharges with q_a=3.9, 2.4 and 1.65.

4. MHD Characteristics of Very Low-q Discharges in DIVA

The plasma column in usual tokamaks are disrupted by so called disruptive instability if the safety factor at limiter q_a becomes low. The large disruption induces a serious electrical and mechanical problems in a large devices. Therefore it is very important to obtain a stable discharge free from large disruptions especially in a large device. Thus number of works have already been devoted to the study of the disruptive instabilities. Various types of precursor oscillations and events immediately preceding the negative voltage spikes are reported and it is shown that the m = 2 mode at the q = 2 surface has a dominant role to fall into the current disruption. Studies on disruptive instability and the precursor mhd activity in very low-q region ($q_a \lesssim 2.5$) are, however, rather few.

This section describes the experimental results of mhd activities especially the disruptive instabilities in very low-q discharges ($q_a \leq 2.5$). It is indicated that the disruptive instability is triggered by large amplitude (typically larger than $\tilde{B}_p/B_p$ = 5 %) m = 2/n = 1 tearing mode near $q_a = 2$. The mode has been excited by radiative cooling in a periphery of the plasma column. In fact, stable discharge with $1.3 \leq q_a \leq 2.5$ has been achieved in DIVA by reducing both metal- and gas-impurities using titanium wall as shown in the previous section. It will be shown that the $q_a < 2$ discharge is free from the major disruptions even if the impurities flow into the plasma.

In subsection 4.1 is devoted to the experimental results of the disruptive instabilities excited by neon injection, and sub-section 4.2 shows the very low q_a discharge, i.e. $q_a < 1$, and results of neon injection into the discharge. Conclusions are given in section 4.3.

4.1 Major Disruptions

In order to observe the disruptive instability in low-q discharges, neon gas is injected into a stable discharge (Fig. 4.1) with $2 < q_a < 2.5$. Discharge characteristics are shown in Fig. 4.2 with and without neon injection. The radiation loss increases from about 15 % of ohmic input power to about 100 % by the neon injection. The disruptive instability is excited with good reproducibility, and the events immediately preceding the negative voltage spike are observed in order to clarify the cause of the disruption. Examples of the loop voltage and the magnetic fluctuation immediately preceding the negative voltage spike are shown in Fig. 4.3. Traces (a) to (d) are cases to lead the major disruption without divertor,

(e) is with divertor and (f) is an example of minor disruption.

Various types of precursor oscillations are observed. The trace (a) shows that a pure m = 2/n = 1 mode gradually grows to lead to negative voltage spike. The amplitude of $\tilde{B}_p/B_p$ reaches 5 % at the negative voltage spike. The trace (b) is an example where the mhd activity is small untill 100 μs before the negative voltage spike. Then m = 2/n = 1 mode rapidly grows up to $\tilde{B}_p/B_p$ = 4 % to lead to a negative voltage spike. In the trace (c) and (d), there is m = 2/n = 1 mode with $\tilde{B}_p/B_p$ = 2 %, and the frequency decreases to stop the rotation or to be damped away (c), then m = 2 mode suddenly grows up to 6 % leading to negative voltage spike.

Operating the divertor the disruption can be also triggered by injecting neon gas but the amount of neon to induce the disruption is 2 ∿ 3 times larger than that without the divertor. The disruptive instability in a plasma with separatrix configuration is shown in trace (e). The behavior of the precursor oscillation is the same as the trace (b). The negative spike appears at $\tilde{B}_p/B_p$ = 4 %. It should be noted that the separatrix does not affect the major disruption. This result extends the previous experiment in high-q discharges.[9)]

The trace (f) is an example of minor disruption, m = 2 mode grows up to $\tilde{B}_p/B_p$ = 2 %, the loop voltage drops slightly but immediately returns, i.e. only the minor disruption is observed.

Figure 4.4 shows an events immediately before and during the negative voltage spikes. About 100 μs before the negative spike, mhd activity gradually increases, and soft x-ray signal at center decreases and at the outer chord slowly increases. This means a spread of a hot column. The events in this phase is the same as minor disruption and/or sawtooth activity. Then m = 2/n = 1 mode suddenly grows up to 5.5 %, and loop voltage drops steeply. The radiation loss including charge exchange loss is 40 kW before the disruption and increases gradually up to 250 kW at the negative voltage spike which is almost equal to the total input power. Figure 4.5 shows profiles of radiative power before the neon injection, just before the negative voltage spkke and after the disruption. These results suggest that internal or minor disruption and impurity cooling enhances the m=2/n=1 mode up to several % which is the source of the negative spike. Therefore the observed behavior of the current disruption in this experiment with $q_a \gtrsim 2$ is very similar to that in high-q discharges.

In the experiment, sadden growth of m=2/n=1 mode is observed, i.e. the level of the mode grows up to 5-7 % during about 30 ∿ 300 μs just before

the disruption. To understand this behavior it is necessary to show how the m=2/n=1 mode grows by the impurity injection. Combining one dimensional transport code and linear helical symmetric tearing code, the observed large m=2/n=1 mode is well simulated as follows. The initial profiles of temperature and density are given from the experimental data. Time development of the radiation loss profile and sawtooth oscillations are also given from the experimental data but other profiles are calculated by the transport code. Saturated level of the m=2/n=1 mode is calculated at any time by the tearing code. Figure 4.6 gives the calculated results, i.e. electron temperature profiles in Fig. 4.6-(a) current profiles in Fig. 4.6-(b) fluctuation level and island width in Fig. 4.6-(c) and the dominant power balance in Fig. 4.6-(d). Plasma near q = 2 is drastically cooled by the radiation loss during 1.5 ms (Fig. 4.6-(a)) and sudden growth of m=2/n=1 mode is observed after the drastic cooling (Fig. 4.6-(c)) because of the change of the current profile (Fig. 4.6-(b)). The level of the m=2/n=1 mode is 5.5 % at 1.5 ms after the injection and the island width is 28 % of the plasma radius (Fig. 4.6-(d)). The large m=2/n=1 flactuations seem easy to disrupt the plasma, which may be combined by m=1/n=1 mode. The radiation loss is almost equal to the total input power at 1.5 ms from the injection. These characteristics obtained from the calculations are very similar to those observed in the experiment. It should be noted that these numerical results are obtained in the case with both the sawtooth oscillations and the impurity injection. The calculated level of the m=2/n=1 mode with only sawtooth oscillations or only impurity injection is a few times less than the observed level.

In conclusion, the direct cause of the disruptive instability is mainly the large m=2/n=1 mode induced by the impurity injection and the internal disruption. From this conclusion, the control of the m=2/n=1 tearing mode is necessarly to supress the disruptive instability. The best way to supress the m=2 mode is to achieve a $q_a < 2$ discharge, because there is no $q_a = 2$ resonance surface in the plasma. Other modes, however, have a possibility to cause the major disruption with $q_a < 2$. Therefore it is very important to achieve a $q_a < 2$ discharge to clarify whether the other mode (for examples m=1/n=1, and m=3/n=2) triggers the major disruption. The result shown in this section suggests that the impurity cooling induces the major disruptions and reduction of the radiation loss is one of the most possible method to obtain $q_a < 2$ discharge.

4.2 Discharges in $q_a < 2$ Region

A discharge in $q_a < 2$ region is very attractive not only to accomplish a high-β tokamak but also to obtain a stable discharge free from current disruptions as discussed in the previous section. Disruptive instability has stood, however, in the way of $q_a < 2$ region, and that has not been stably achieved. In DIVA, the discharges in $q_a < 2$ region has been stably obtained by reducing a radiation loss.

An example of the discharge is shown in Fig. 4.7. When the discharge falls into $q_a < 2$ region, fluctuations including m=3/n=2 are observed by magnetic probes but the level is very low, i.e. $\tilde{B}_p/B_p = 0.05$ %. Large sawtooth oscillations are observed in soft x-ray signal and loop voltage and the energy replacement time τ_E is dominated by these internal disruptions. The average energy confinement time, however, follows Alcator scaling with an higher numerical factor in front of $a^2 n_e q_a^{1/2}$. Therefore $q_a < 2$ discharge with good confinement property is obtained as discussed in section 3. Reduction of the radiation loss has dominant role to obtain $q_a < 2$ discharges. The sum of the radiation loss and the charge exchange loss is 32 kW for 280 kW joule input in the case of Fig. 4.7 and the $Z_{eff} \simeq 1$.

During the initial current rise phase of the discharge, several times of voltage rise appear at which the safety factor at limiter q_a crossing an integer value. Enhanced mhd activities are observed when the voltage rises appear, and then the mode numbers correspond usually to q_a. An Expanded trace of $\tilde{B}_p$ and loop voltage are also shown in Fig. 4.7.

When the plasma current is crossing through $q_a = 2$, $m = 2/n = 1$ which may be kink mode grows up, to $\tilde{B}_p/B_p = 4$ % and the loop voltage rises, but negative voltage spike is not usually observed. The characteristics feature of the mhd activity is not changed by changing the current rising time from 2.5 to 6 ms. When the plasma has a separatrix in the shell, i.e. the divertor, the duration of voltage increase is shorter than the case without divertor, and the mhd activity is much smaller than that without the divertor by a factor of 4 as shown in Fig. 4.8. Therefore the separatrix stabilizes the kink mode.

The ratio of radius of the shell to the limiter $\bar{b}/\bar{a}$ is 1.2 in the case of Figs. 4.7 and 4.8. If the limiter is inserted to $\bar{b}/\bar{a} = 1.35$, a stable $q_a < 2$ discharge can be obtained only during $3 \sim 5$ ms without divertor and the plasma column is shifted outward of the torus and disrupted because of no control field. This behavior is observed also in a high-q discharge with $\bar{b}/\bar{a} = 1.35$. The mhd activity is weaker in a $q_a < 2$ discharge than in

high-q discharge even with $\bar{b}/\bar{a}$ = 1.35. The result suggests that the plasma with $\bar{b}/\bar{a}$ = 1.35 can be stably obtained with a suitable control field. Figure 4.9 shows an example of q_a < 2 discharge with $\bar{b}/\bar{a}$ = 1.3 and the divertor. In this case, iron core is saturated and a q_a < 2 discharge is obtained during only 4 ms.

An example of neon injection into the $q_a \sim 2$ discharge is shown in Fig. 4.10. The radiation loss including charge exchange loss is about 30 kW before neon injection and increases up to 250 kW by the injection in all cases. It should be noted that no disruptive instability occurs in q_a < 2 region which is contrast with disruptions in q_a > 2 region as shown in Fig. 4.10.

When neon gas is injected into stable q_a = 1.6 discharges. The loop voltage increases as increasing radiation loss, and the plasma current decreases because of increase of resistivity. After the safety factor q_a becomes larger than two, a mhd activity grows and the first major disruption occurs at q_a = 2.2 in this case shown in Fig. 4.11. The number of observed disruptions at different q_a values are shown in the same Fig. 4.11. Disruptions are frequently observed near q_a = 2. It should be noted that the disruptive instability does not appear in q_a < 2 region.

4.3 Conclusion

Following results are obtained in the low-q experiment.

1) Large m=2/n=1 fluctuations induced by impurity injection and by internal disruption is the direct course of the major disruption with $q_a \gtrsim 2$.
2) Separatrix does not affect the major disruption.
3) Reducing impurity level, the q_a < 2 discharges are stably obtained with $\bar{b}/\bar{a}$ = 1.2 and probably $\bar{b}/\bar{a}$ = 1.35.
4) Increase of loop voltage and m=2/n=1 mode, probably kink mode, are observed when q_a is near 2. The fluctuation level of the mode is reduced by the separatrix magnetic surface.
5) Internal disruptions are observed but the major disruption cannot be exited in the q_a < 2 discharges.

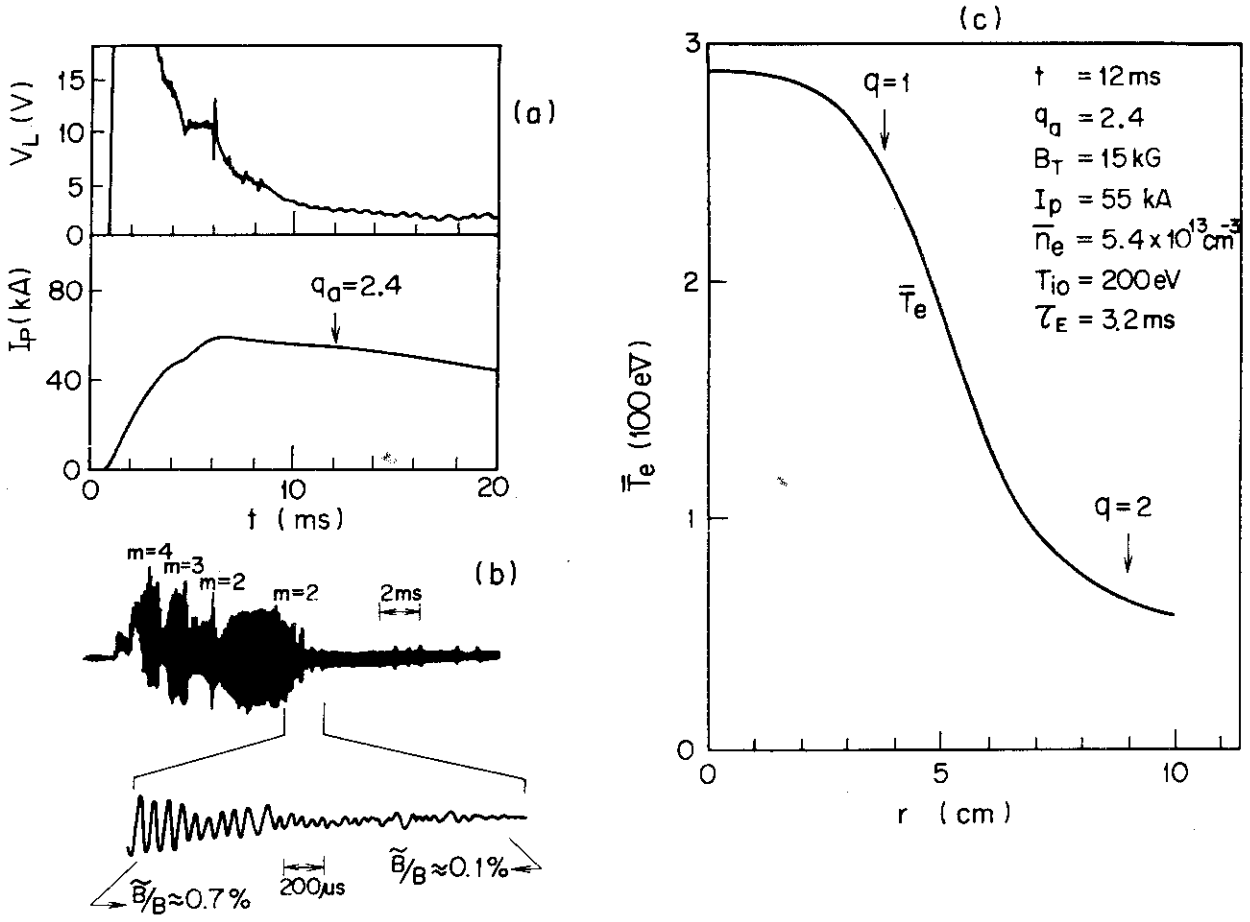

Fig. 4.1 Typical stable low q discharge ($2.5 > q_a > 2$)

(a) Oscillogram of loop voltage V_L and plasma current I_p. Small sawtooth activity appears on the loop voltage after about 10 ms.

(b) Oscillogram of mhd activity $\tilde{B}_p$ with scanning time of 2 ms, and oscillogram of mhd activity $\tilde{B}_p$ with scanning time of 200 μsec from 10 ms to 12 ms. Enhanced mhd activity are observed during the current rise phase, of which mode numbers correspond usually to q_a. Positive perturbations of loop voltage appear corresponding to the above mentioned mhd activity. However, after the sawtooth activity appears on the loop voltage, mhd activity becomes very low ($\tilde{B}_p/B_p \sim 0.1$ %) of which mode number is m=2/n=1.

(c) Electron temperature profile and typical plasma parameters at 12 ms.

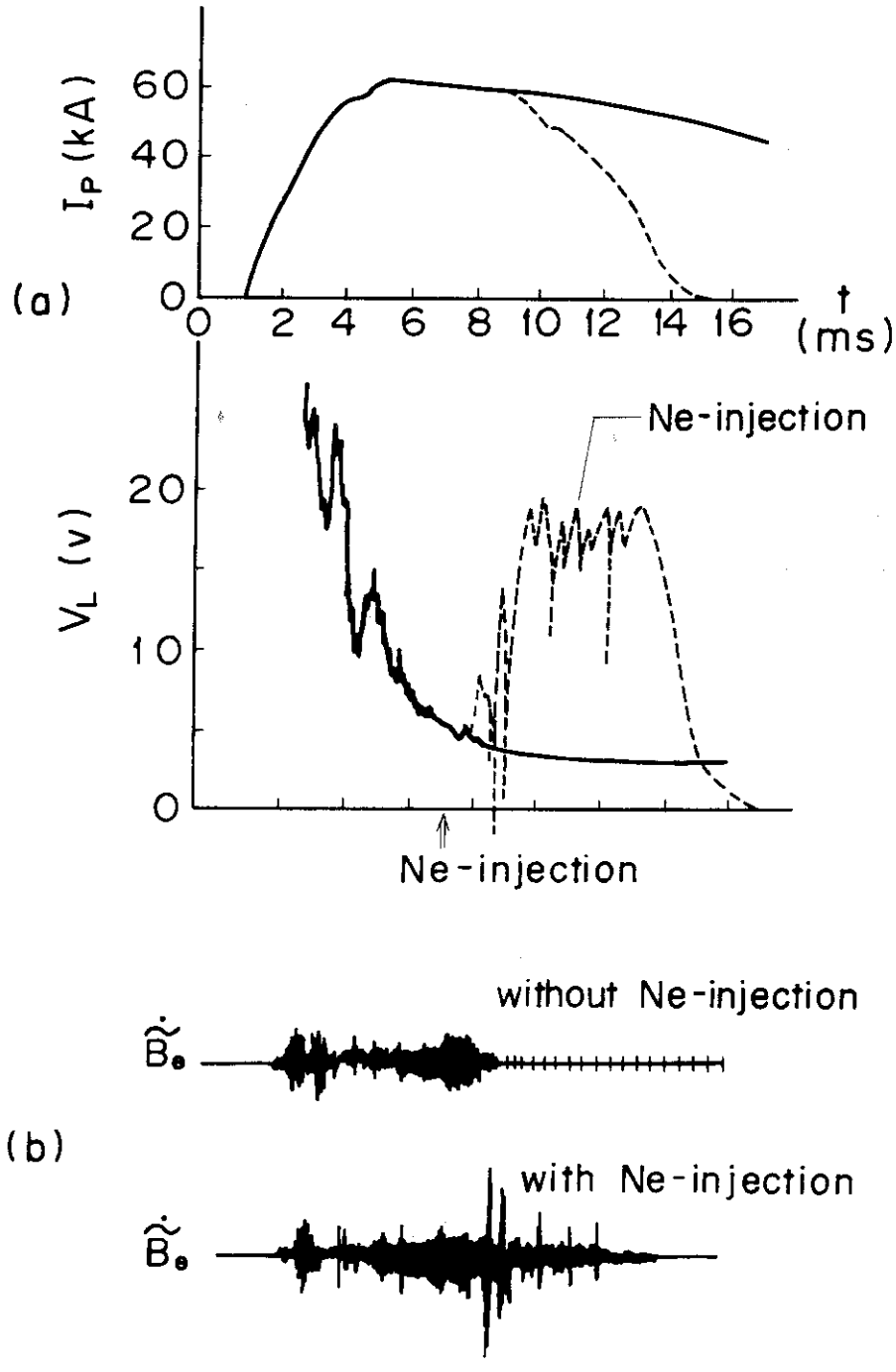

Fig. 4.2 Discharge characteristics of low q ($q_a \sim 2.2$) discharge with and without neon injection. Neon is injected at 7 ms with time duration of about 1 ms. The relation loss increases from about 15 % of ohmic input power to about 100 % by the neon injection.

(a) Oscillogram of loop voltage V_L and plasma current Ip. Solid line (-) shows the case without neon injection and broken lines (---) show the case without neon injection.

(b) Oscillogram of mhd activity $\tilde{B}_P$ with and without neon injection.

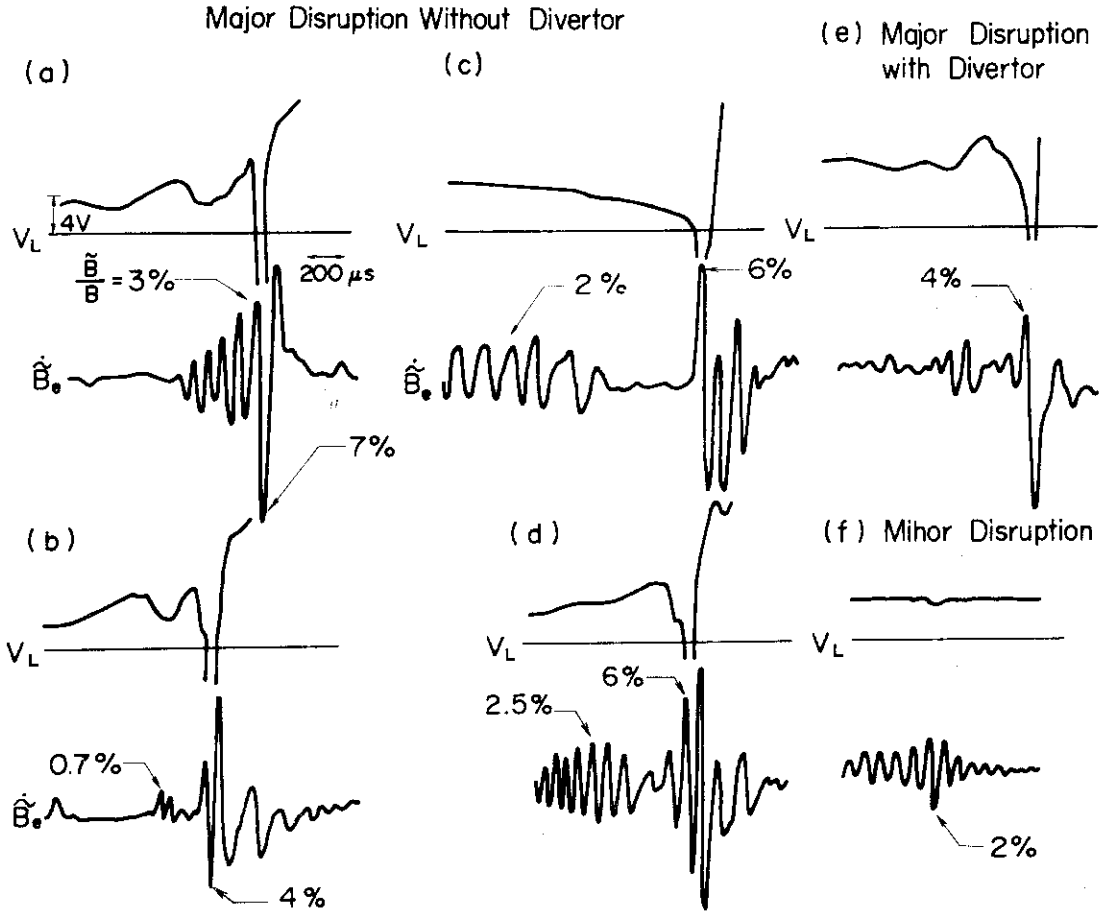

Fig. 4.3 Examples of the loop voltages and mhd activities immediately preceding the negative voltage spike with the neon injection. Trace (a) to (d) are cases to lead the major disruption without divertor, while (e) is with the divertor. Trace (f) is an example of minor disruption without divertor.

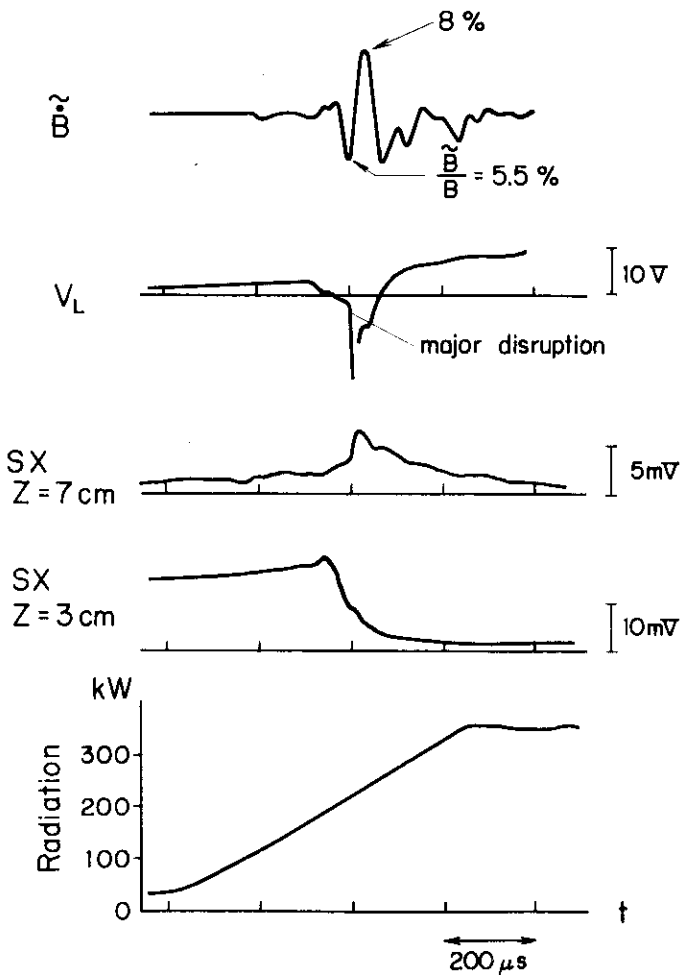

Fig. 4.4 Evolution of mhd activity $\tilde{B}_p$, loop voltage V_L, soft X-ray signal of two different chords, and total radiation loss during the disruptive instability. q = 1 surface is located at about r = 5 cm before disruption.

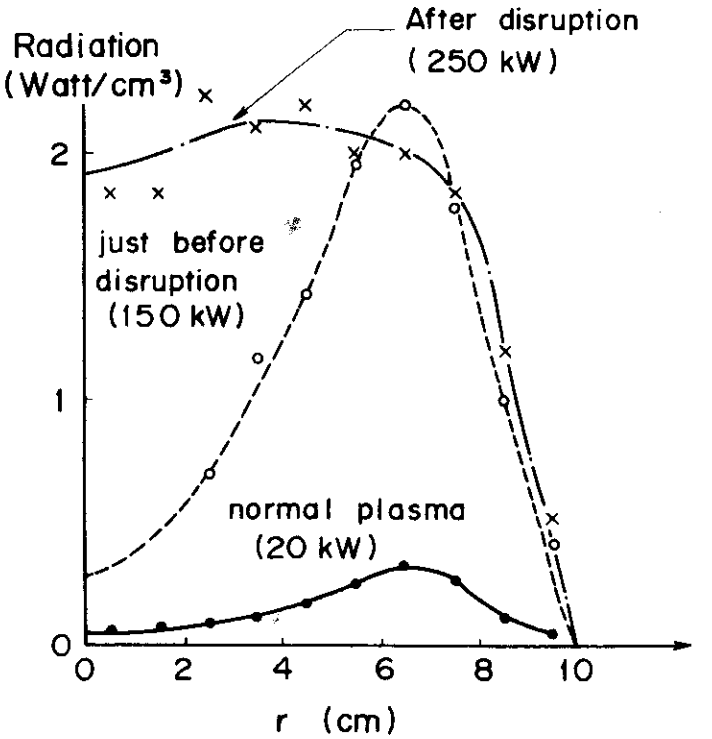

Fig. 4.5 Radial profile of radiation loss just before and after the disruption with the neon injection. Radial profile of radiation loss without neon injection is also depicted in order to compare the profile without injection to that with the injection.

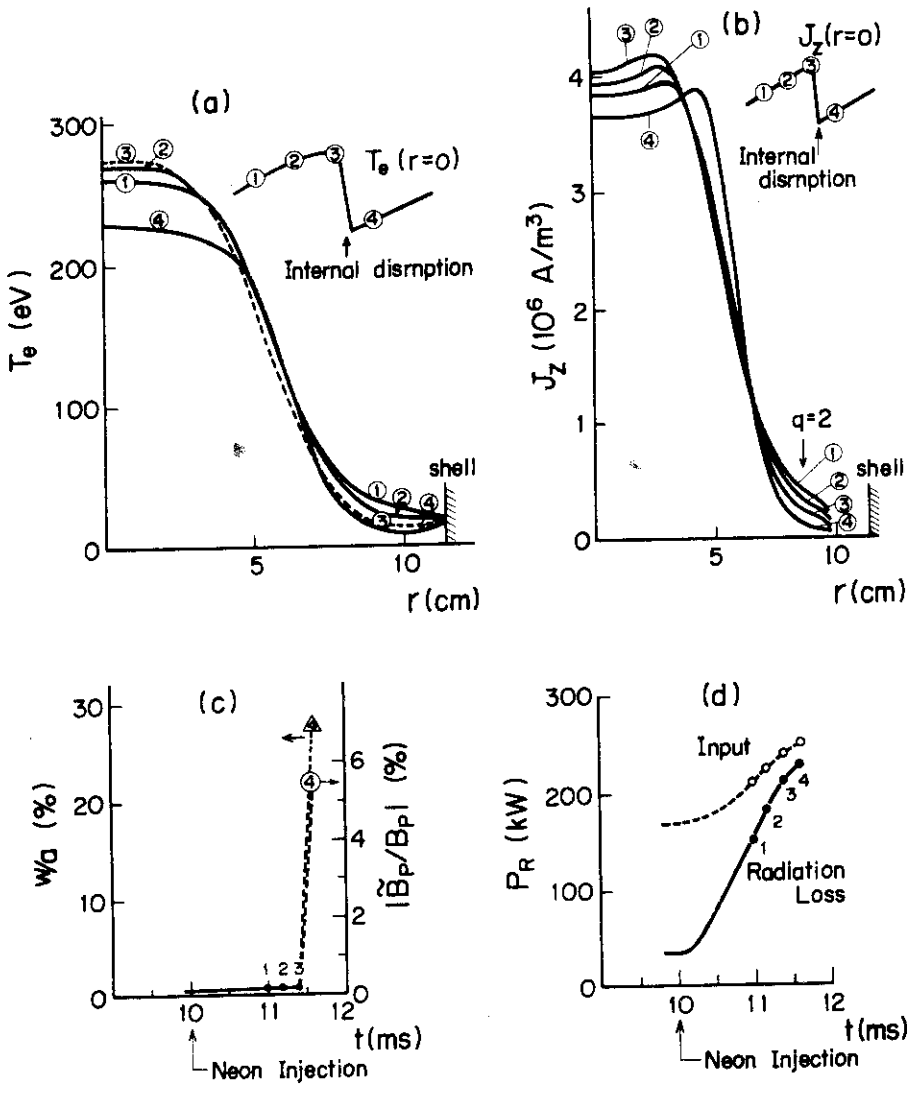

Fig. 4.6 Numerical results of fluctuation level and the island width of the m-2/n=1 tearing mode with the neon injection. Calculations are performed combining one dimensional transport code and linear helical symmetric tearing code.

(a) Time evolution of temperature profiles from the start of neon injection to the disruption, plotted at 250 μsec spacings. The initial temperature and density profiles are given from the experimental results. Time evolution of the radiation loss profile and repetition time of sawtooth oscillation (500 μs) are also given from the experimental data but other profiles are calculated by the transport code.

(b) Corresponding time evolution of current profile

(c) Corresponding time evolution of fluctuation level $\tilde{B}_p/B_p$ and normalized with W/a of m=2/n-1 tearing mode.

(d) Corresponding time evolution of Joule input and total radiation power.

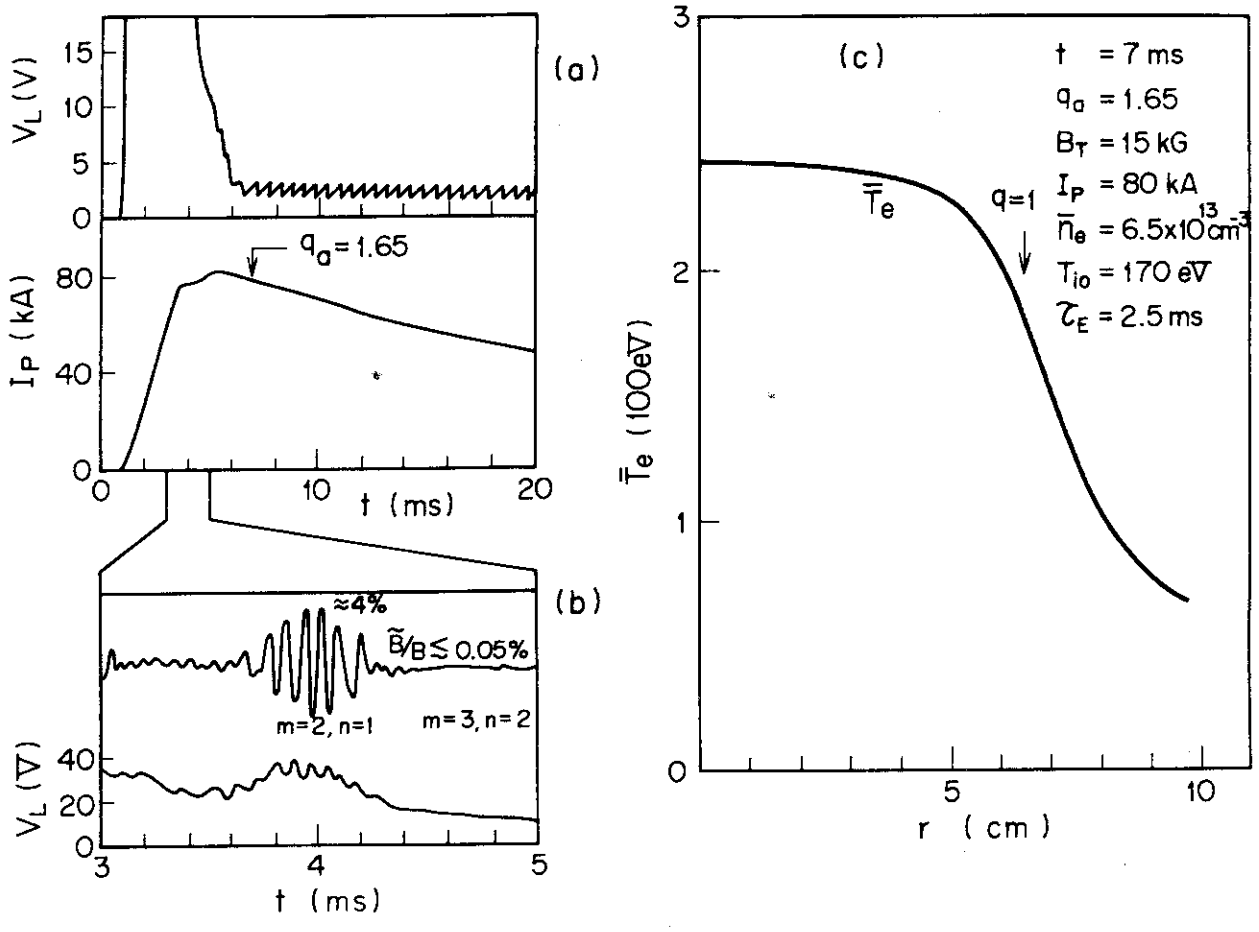

Fig. 4.7 Typical stable low-q discharge (q < 2)

(a) Oscillogram of loop voltage V_L and plasma current Ip. Large sawtooth activity appears on the loop voltage after about 6 ms.

(b) Oscillogram of mhd activity $\tilde{B}_P$ with scanning time of 200 s.
Enhanced mhd activity is observed, when the plasma current is crossing through q_a = 2, of which mode number is m=2/n=1. Positive perturbations of loop voltage appear corresponding to the above mentioned mhd activity. However, after the sawtooth activity appears on the loop voltage, mhd activity becomes very low ($\tilde{B}_P/B_P \lesssim 0.05$ %).

(c) Electron temperature profile and typical plasma parameters at t = 7 ms.

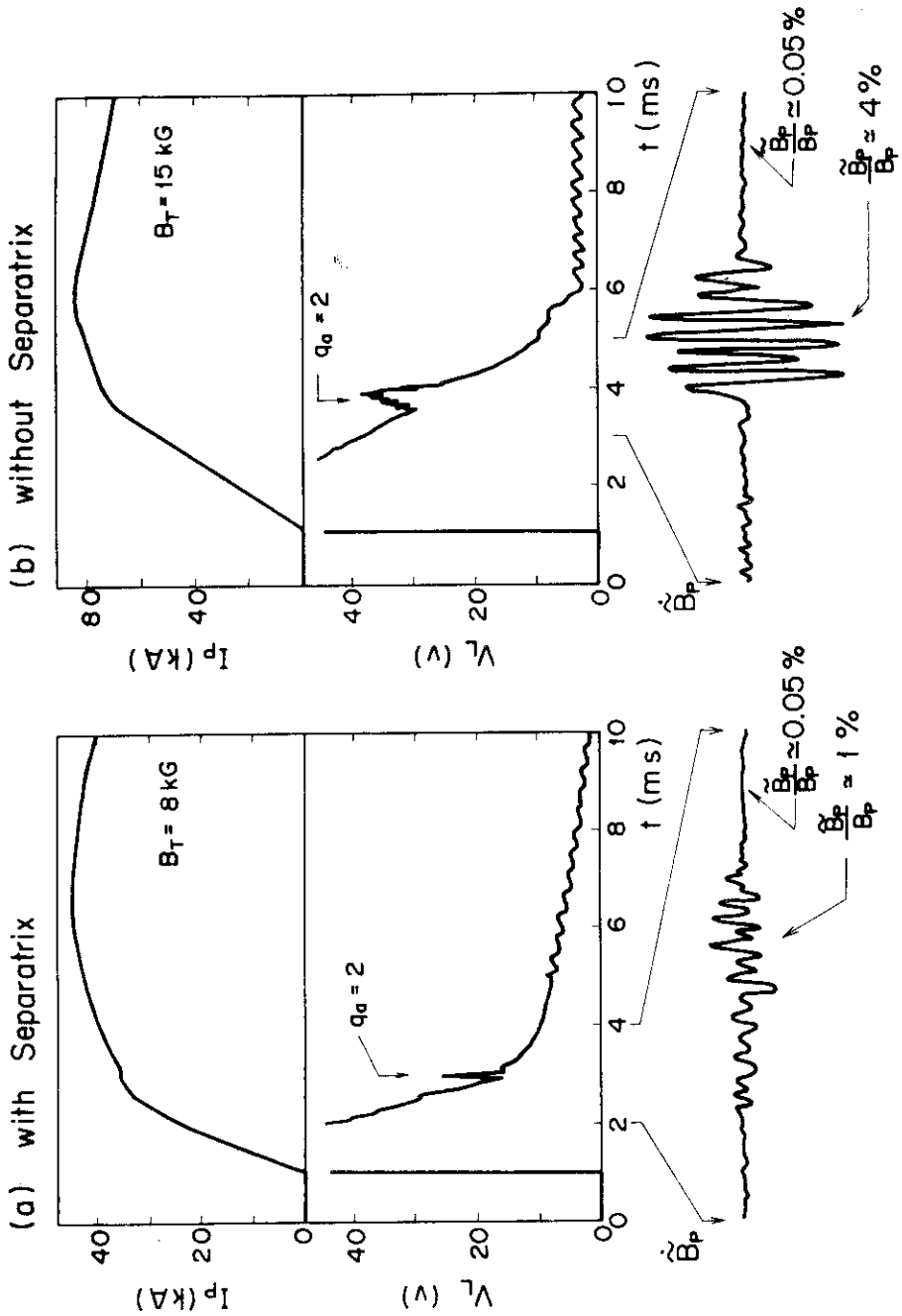

Fig. 4.8 Oscillogram of plasma current Ip and loop voltage V_L with scanning time of 2 ms, and oscillogram of mhd activity with scanning time of 200 μs, during the current rize phase for two discharges with an without separatrix. These figures show separatrix has a stabilizing effects on the surface mode.

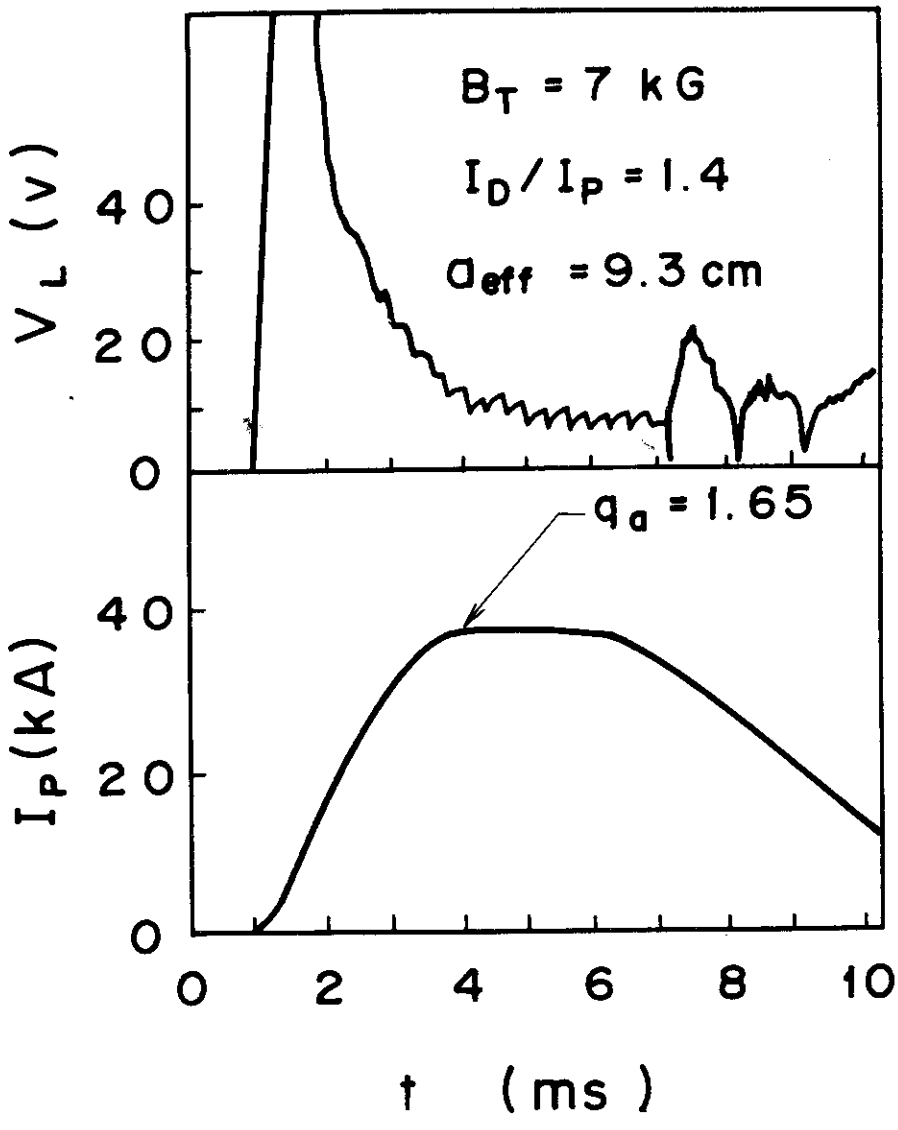

Fig. 4.9 Evolution of loop voltage V_L and plasma current Ip in the case of $q_a < 2$ discharge with the divertor and $\bar{b}/\bar{a} = 1.35$. A stable discharge is obtained during $q_a < 2$.

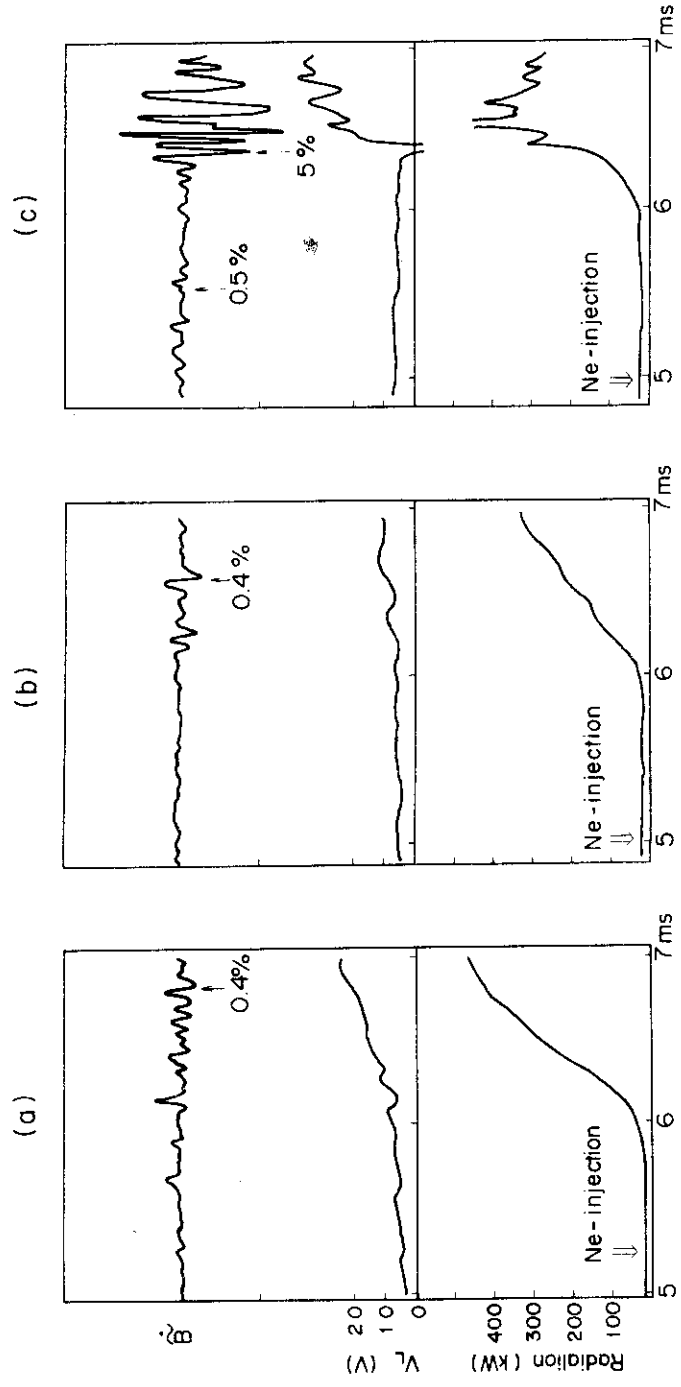

Fig. 4.10 Evolution of mhd activity $\tilde{B}_\theta$, loop voltage V_L and total radiation loss in the cases of neon injected into three different discharges with the safety factor $q_a \sim 2$. The radiation loss including charge exchange loss is about 40 kW before neon injection and increases up to 250 kW by the injection in all cases. These figures show that the major disruption does not occur when the safety factor q_a is less than 2.

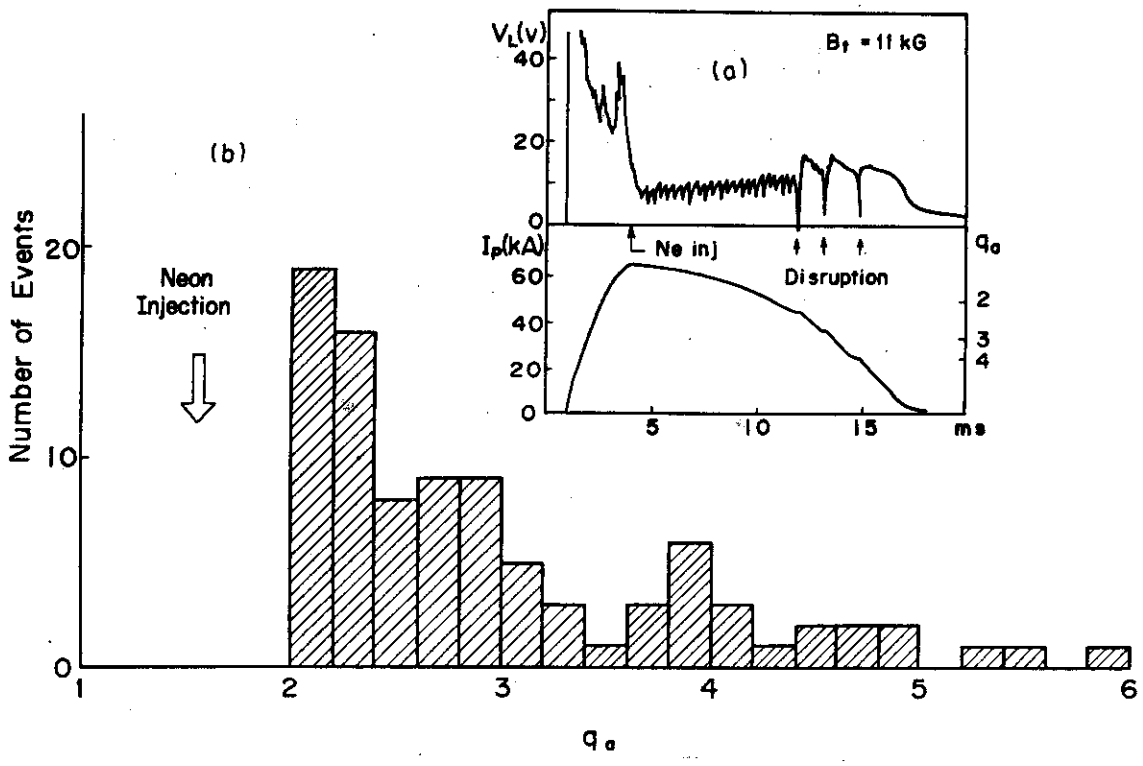

Fig. 4.11 Typical plasma parameters and number of occurrence of observed disruptions at different q_a when the neon is injected into the stable q_a = 1.6 discharge.
Major disruptions do not occur when the safety factor q is less than 2.

(a) Time behavior of loop voltage and plasma current with neon injection at 4 ms into the stable q_a = 1.6 discharge. The loop voltage increases at increasing radiation loss, and the plasma current decreases due to increasing resistivity. After the safety factor q_a becomes larger than two, the first major disruption occurs, and a series of voltage spikes appears on the loop voltage.

(b) The number of occurrence of observed disruption at different q_a.
Disruptions are frequently observed near q_a = 2.

5. Summary

The following results are obtained in very-low-q discharges.

1) Stable plasmas with a good confinement properties are obtained with $1.3 \leq q_a < 2$.
2) A $q_a \gtrsim 1$ discharge has a poor confinement time.
3) Non circular configuration inside a plasma column is obtained in the very-low-q discharges.
4) Energy confinement time can be improbed by a factor of a few in very-low-q discharges if the internal disruption is suppressed.
5) Modified Alcator scaling, i.e. $\tau_E \propto a_{half}^2 \bar{n}_e q_a^{1\ 2}$, describes well observed confinement time of various discharge conditions without large mhd activities.
6) Plasma-wall interactions due to the internal disruption has a possibility to enhance serious impurity efflux in a large device.
7) Large m-2/n-1 fluctuations induced by impurity injection is the direct trigger of the major disruption with $q_a \lesssim 2$.
8) Separatrix does not affect the major disruption.
9) Reducing impurity level, the $q_a < 2$ discharges are stab ly obtained with $\bar{b}/\bar{a} = 1.2$ and probably $\bar{b}/\bar{a} = 1.35$.
10) Increase of loop voltage and m=2/n=1 mode, probably surface mode, is observed when q_a is near 2. The fluctuation level of the mode is reduced by the separatrix magnetic surface.
11) Internal disruptions are observed but the major disruption cannot be exited in the $q_a < 2$ discharges.

Very-low-q discharges free from major disruptions are obtained with a good confinement property. The results 4) and 6) show that suppression of sawtooth oscillations is important and desirable to obtain much more improved tokamak plasma.

The most important and interesting result in the mhd study is "the major disruption cannot be excited in the $q_a < 2$ discharge." This result shows that the other fluctuations except m=2/n=1, e.g. m=3/n=2, m=4/n=3 and even m=1/n=1, cannot induce the major disruption in very low-q discharges. The reason why only the m=2/n=1 tearing mode can excite the disruption is not understood but the following consideration is consistent with the result. A tearing mode of $n \neq 1$ has a poor growth rate and may not directly induce the major disruption. The m=1/n=1 mode has a large growth rate and

grows mainly inside of the q = 1 surface. But the m-2/n=1 mode grows in the both sides of the q = 2 surface. This difference between m=1/n=1 and m=2/n=1 may explain that the m-1/n=1 induces the internal disruption and the m-2/n=1 the major disruption. In extremely-low-q discharges with $q_a \gtrsim 1$ the m=1/n=1 mode can grow to the plasma surface and has a possibility to induce the major disruption. But no disruption is observed even near $q_a = 1$. This result may be explained as follows: The profiles of the plasma energy density and/or current density are almost flat near $q_a = 1$ and energy source is not sufficient to induce the major disruption. Detailed investigations including numerical study, however, are necessary to understand the experimental result, i.e. no major disruption can be excited in $q_a < 2$ discharges.

The other important and interesting feature is a possibility to operate the very low-q discharge in a large tokamak because the above result encourages the attempt to achieve a high-β tokamak free from the dangerous major disruption. However the following questions arise in a large tokamak.

a) Conditions for obtaining the $q_a < 2$ discharge.
b) Conditions for maintaining the $q_a < 2$ discharge.

Concerning the first condition, it is necessary to discuss the major disruption due to the m=2/n=1 tearing mode and kink mode near $q_a = 2$. The tearing mode has to be stable if the plasma current and pressure have suitable profiles which are obtained by reducing radiation loss in DIVA and can be obtained by controlling input and/or impurity profiles in a large tokamak. The surface mode has a possibility to disrupt the plasma column at $q_a \gtrsim 2$. This mode can be stabilized by a close shell and also by a close resistive shell.[10] In DIVA, the $q_a < 2$ discharge is stably obtained with $\bar{b}/\bar{a} = 1.2$. This value seems easily to be obtained in a large tokamak. For example in JT-60, $\bar{b}/\bar{a} \lesssim 1.1$ and the time constant of the vacuum chamber is a few tens ms for low-m mode. Therefore the $q_a < 2$ discharge seems easily obtained in a large tokamak. In DIVA, however, a scrape-off plasma with $T_e \geq 20$ eV and $n_e \geq 3 \times 10^{12}$ cm^{-3} is observed in a shadow of the limiter and has a possibility to stabilize the surface mode. Therefore it is very important to know the effect of the scrape-off plasma and to estimate a scrape-off plasma obtained in a large device. If the effect is strong and a suitable scrap-off plasma is not obtained in a large tokamak, it seems difficult to obtain the $q_a < 2$ discharge in a large tokamak. Even in this case, the other stabilizing effect that is the stabilizing

effect by the separatrix magnetic surface can be expected. Therefore it seems easy to obtain the $q_a < 2$ discharge in a large device with the separatrix, e.g. JT-60, in which the scrape-off plasma may be more easily controlled than in a conventional tokamak and the separatrix effect can be expected.

After obtaining the $q_a < 2$ discharge, the last problem is how the discharge is stably maintained. From the experimental result, no major disruption occurs. Therefore the problem is the large internal disruption. The internal disruption has to be stabilized if the current profile can be controlled in a large tokamak. If the internal disruption cannot be stabilized, the following problem arises. The internal disruption increases the boundary plasma temperature as observed in the experiment. The loss has possibility to induce the dangerous impurity efflux to a confined plasma as a result of plasma-wall interactions. The heat and particle flux enhanced by the internal disruption may be guided into the divertor because runaway electrons were observed to be guided into the divertor even in unstable discharges.[9] Therefore the enhanced loss is not dangerous in a divertor device. Summarizing the discussions, the $q_a < 2$ discharge seems realistic in a large tokamak especially in a divertor device.

Acknowledgments

The authors are indebted to Dr. M. Wakatani and members of Theoretical group of JAERI for their stimulating and valuable discussions and members of DIVA operation group for their excellent assistance in the experiment. They would like to thank Drs. S. Mori, Y. Obata, M. Yoshikawa and Y. Tanaka for their continuous encouragement.

effect by the separatrix magnetic surface can be expected. Therefore it seems easy to obtain the $q_a < 2$ discharge in a large device with the separatrix, e.g. JT-60, in which the scrape-off plasma may be more easily controlled than in a conventional tokamak and the separatrix effect can be expected.

After obtaining the $q_a < 2$ discharge, the last problem is how the discharge is stably maintained. From the experimental result, no major disruption occurs. Therefore the problem is the large internal disruption. The internal disruption has to be stabilized if the current profile can be controlled in a large tokamak. If the internal disruption cannot be stabilized, the following problem arises. The internal disruption increases the boundary plasma temperature as observed in the experiment. The loss has possibility to induce the dangerous impurity efflux to a confined plasma as a result of plasma-wall interactions. The heat and particle flux enhanced by the internal disruption may be guided into the divertor because runaway electrons were observed to be guided into the divertor even in unstable discharges.[9] Therefore the enhanced loss is not dangerous in a divertor device. Summarizing the discussions, the $q_a < 2$ discharge seems realistic in a large tokamak especially in a divertor device.

Acknowledgments

The authors are indebted to Dr. M. Wakatani and members of Theoretical group of JAERI for their stimulating and valuable discussions and members of DIVA operation group for their excellent assistance in the experiment. They would like to thank Drs. S. Mori, Y. Obata, M. Yoshikawa and Y. Tanaka for their continuous encouragement.

* DIVA Group

Arrangement	Y. Shimomura H. Maeda
Fluctuation (magnetic probe)	M. Nagami K. Odajima
Fluctuation (PIN diode)	S. Yamamoto S. Sengoku
Heating and power balance	K. Odajima H. Kimura S. Sengoku
Microwave interferometory	A. Funahashi K. Takahashi H. Ohasa
Neutral particle energy analysis	H. Takeuchi K. Kakahashi
Plasma-wall interactions	S. Sengoku H. Ohasa S. Yamamoto
Scrape-off layer plasma	H. Kimura K. Odajima
Spectroscopy	S. Kasai T. Sugie M. Nagami
Surface observation	H. Ohasa H. Ohtuka
Thomson scattering	T. Yamauchi K. Kumagai S. Sengoku
X-Ray (hard, PIN)	S. Yamamoto S. Sengoku
X-ray)soft)	K. Kumagai
Computer simulation	M. Azumi M. Nagami S. Sengoku
Data processing	A. Shoji T. Kawakami
Operation and engineering group of DIVA	K. Anno T. Shibata H. Hiratsuka H. Sunaoshi K. Yokoyama

References

1) VLASENKOV, V.S., LEONOV, V.M., MEREZHKIN, V.G., MUKHOVATOV, V.S., Third internal symposium on toroidal plasma continement, (Garching, 1973).
2) DIVA Group, Nuclear Fusion, 18 (1978) 1619.
3) MAEDA, H., SENGOKU, S., KIMURA, H., OHTSUKA, H., OHASA, K., et al., 7th International Conference on Plasma Physics and Controlled Nuclear Fusion Research (Insbruck, 1978) paper T-3-1.
4) SHIMOMURA, Y., NAGASHIMA, T., KITSUNEZAKI, A., MAEDA, H., OHTSUKA, H., et al., The First Results on JFT-2a, Japan Atomic Energy Research Institute Report JAERI-M 6102 (1975).
5) NINOMIYA, H., private communication.
6) MURAKAMI, M., CALLEN, J.D., BERRY, L.A., Nuclear Fusion 16 (1976) 347.
7) FIELDING, S.J., HUGILL, J., McGRACKEN, G.M., et al., Nuclear Fusion 17 (1977) 1382.
8) JFT-2 Group, private communication.
9) SHIMOMURA, Y., MAEDA, H., OHTSUKA, H., KITSUNEZAKI, A., NAGASHIMA, T., Phys. of Fluids, 19 (1976) 1635.
10) TANAKA, M., TUDA, T., TAKEDA, T., Nucl. Fusion 13 (1973) 119.